LANGMUIR

pubs.acs.org/Langmuir Article

Self-Organization of Mobile, Polyelectrolytic Dendrons on Stable, Amphiphile-Based Spherical Surfaces

Akash Banerjee and Meenakshi Dutt*



Cite This: Langmuir 2023, 39, 3439-3449



ACCESS

III Metrics & More

Article Recommendations

Supporting Information

ABSTRACT: Spherical surfaces bearing mobile, solvophilic chains are ubiquitous. These systems are found in nature in the form of biological cells bearing carbohydrate chains, or glycans, or in drug delivery systems such as vesicles bearing polyethylene glycol chains and carrying therapeutic molecules. The self-organization of the chains on the spherical surface dictates the stability and functionality of the latter and is determined by key factors such as the interchain, chain—surface interactions, excluded volume, concentration of the chains, and external environment. This study develops a fundamental understanding of how these factors control the organization of mobile, solvophilic chains while preserving the stability of the spherical surface. To that end, the study focuses on the organization of polyamidoamine dendrons on the surface



of a dipalmitoylphosphatidylcholine-based vesicle. The excluded volume of the chains and the external environment are, respectively, controlled via the dendron generation and the pH. For acidic and basic pH environments, the dendrons are extended away from the surface. As a consequence, the vesicles are able to accommodate significantly higher concentration of dendrons on their surface without rupturing. For acidic pH, the dendrons change their conformation to avoid intermeshing. However for basic pH, the dendrons only change their conformation at extremely high concentrations due to excluded volume effects. These conformational changes are attributed to the number of protonated dendron residues that vary as a function of pH. The results from this study will advance diverse subdisciplines within cell biology, biomedicine, and pharmaceuticals.

INTRODUCTION

Spherical surfaces with mobile, solvophilic chains in the aqueous environment are ubiquitous. 1-3 The chains are grafted to a molecule which is embedded and freely diffusing within the spherical surface. Such systems are found in nature in the form of biological cells with sugar chains, or glycans, on their surface to enable critical physiological functions such as cellcell communication, protein folding, or defensive responses to bacterial infections.^{3,4} Another example is vesicles bearing polyethylene glycol (PEG) chains (namely, PEGylated vesicles) on their surface for use in the delivery of therapeutics. 5,6 The presence of PEG chains endows interfacial stability to the vesicles while significantly prolonging their circulation time. In spite of the distinct chemistry of the chains in the two examples, their functionality is dependent upon key factors including the interchain, chain-surface interactions, excluded volume, concentration of the chains, and external environment. 5,7-9 Furthermore, the self-organization of these chains on a spherical surface determines the stability of the surface. For example, a high concentration of PEG chains on the surface of a lipid vesicle will result in its rupture due to the asymmetric stresses induced by the excluded volume of the chains.5 Given the ubiquity of these systems in nature and consumer goods, it is critical to develop a fundamental understanding of how these key factors control the

organization of these mobile chains on spherical surfaces without disrupting the stability of these surfaces. To that end, this study elucidates the impact of the key factors on the selforganization of mobile polyamidoamine (PAMAM) dendrons on the surface of a dipalmitoylphosphatidylcholine (DPPC)based vesicle. The PAMAM dendrons are grafted to two alkyl chains which are chemically identical to the hydrocarbon chains in DPPC. 10,11 This system has been selected as it is deemed ideal to probe the key factors determining the stability of the vesicles decorated with mobile, solvophilic chains. The external environment varied via the pH of the system. The results from this study have the potential to accelerate the development of a wide range of disciplines including biochemistry, cell biology, immunology, and pharmaceutical sciences with the goal of enabling new technologies for the advancement of health care.

Received: December 17, 2022 Revised: February 12, 2023 Published: February 21, 2023





Prior experimental studies on spherical surfaces with mobile, solvophilic chains in the aqueous environment include PEGylated vesicles, 5,6 dendronized vesicles, 10,11 and various types of lipid nanoparticles.1 These studies investigate the impact of features such as the length, concentration of the solvophilic chain, and pH on the stability of the vesicles. For example, a study on PEGylated vesicles reports that a high concentration of PEG chains are required for the colloidal stability of the vesicles.⁵ However, an extremely high concentration of PEG chains ruptures the vesicles. In another study, vesicles encompassing pH-responsive solvophilic chains disaggregate into small micelles under acidic conditions. 11 This enables controlled release of the therapeutic cargo into the cytosol of biological cells. Other experimental studies report that the conformation of the solvophilic chains determines the functionality of these systems.8 These studies underscore the need to resolve the mechanisms that govern both the stability and functionality of spherical surfaces decorated with mobile, solvophilic chains. Computational studies complement these experimental results by elucidating the molecular characteristics of these complex systems.

The formation and equilibrium morphology of vesicles encompassing phospholipids and amphiphiles with linear, solvophilic chains have been examined under bulk conditions and volumetric confinement using computational approaches.^{9,12,13} The linear, solvophilic polymer chains were mobile on the surface of the vesicles and did not have any favorable interactions with the phospholipid head groups. These studies have examined the effect of the length and concentration of the chains using different simulation techniques including molecular dynamics (MD), ¹³ MD-lattice Boltzmann, ⁹ and dissipative particle dynamics. ¹² The chains were observed to spatially distribute themselves uniformly across the vesicle surface. Furthermore, a lower concentration of the solvophilic chains with longer lengths formed stable vesicles. 12 Theoretical calculations and self-consistent field theory simulations examined the conformation of dendrons grafted on spherical surfaces as a function of their curvature, the generation of the dendrons, ¹⁴ and solvent quality. ¹⁵ The dendrons were not mobile on the surface or attributed any effective chemical properties and thereby did not have any interactions with neighboring dendrons or the surface.

This study elucidates the self-organization of PAMAM dendrons on the surface of stable DPPC vesicles. The PAMAM dendrons are part of polyamidoamine dendrongrafted amphiphiles (PDAs). The PAMAM dendrons are grafted to two alkyl chains that are identical to the hydrocarbon tails in DPPC. Due to considerations of the computational efficiency, the dynamics of the system are probed using coarse-grained (CG) MD simulations. The organization of the dendrons on the vesicle is examined as a function of key factors such as the interactions, excluded volume, concentration of the dendrons, and the pH of the external environment. Furthermore, the study identifies the highest, or critical, concentration of the PDAs which yield stable spherical surfaces. The results from this study demonstrate that the intricate balance between the key factors determines the self-organization of the mobile, polyelectrolytic dendrons on stable spherical surfaces. These results will aid in the elucidation of fundamental mechanisms, underlying the conformation of glycans on the surface of biological cells. From a technological perspective, the results from this study can potentially inspire and inform the design and synthesis of the new amphiphiles, which are integral constituents of vehicles for delivery of therapeutics, ^{16–18} vaccines, ^{1,19,20} or enhancing immune defenses within a host.

MATERIALS AND METHODS

Vesicles encompassing mixtures of DPPC lipids and PDAs are investigated. This study builds upon a previous study²¹ and elucidates the properties of these vesicles for acidic and basic pH conditions. DPPC lipids and PDAs are amphiphiles with identical hydrophobic segments encompassing two alkyl chains each. The hydrophilic segments of a PDA molecule, also known as the head groups, consists of primary, tertiary amines, and amides. These head groups are organized as a hyper-branched polymer and are called dendron branches. A DPPC lipid molecule has two head groups, namely, phosphate and choline groups. DPPC lipids have been extensively studied using both experimental²²⁻²⁴ and computational approaches.²⁵⁻²⁷ DPPC lipids are suitable for making stable vesicles as they are in the gel state at physiological temperatures. 5,22-24,28 Furthermore, mixtures of DPPC lipids and amphiphiles with bulky head groups (like the ones used in this study) also form stable vesicles in aqueous solution.²⁹ Vesicles are created by varying the relative concentration and generation (G1 through G5) of the dendrons. The characteristics of these vesicles are determined at acidic and basic pH. The dynamics of the systems is resolved using the MD simulation technique. Since these systems span large spatial (50 nm) and temporal [5000 nanoseconds (ns)] scales, the CG MARTINI force field³⁰ is employed to reduce computational runtimes. An explicit representation of water is used to accurately solvate the dendron branches. The non-bonded interactions are defined by the Lennard-Jones and Coulombic potentials with a 1.2 nm cutoff. Long-range electrostatics using techniques such as particle mesh Ewald (PME) summation 31,32 is not employed due to the large system sizes. In an earlier study on dendronized vesicles, 21 it is shown that the inclusion of PME does not significantly impact the results.

The CG model for DPPC lipids is adopted from the MARTINI lipid repository. ³³ Each alkyl chain of the PDA and DPPC molecules encompasses C1 MARTINI beads. The DPPC head groups (phosphate and choline) are represented by Q_a (unit negative charge) and Q_0 (unit positive charge) MARTINI beads, respectively. The CG model for the PDA molecules is based on its atomistic structure reported in an experimental study. ¹¹ This molecule consists of a dendron (head group) that is grafted to two alkyl chains. The CG model for the dendrons is adopted from a MARTINI-based study on dendrimers (a dendron is half of a dendrimer). ^{34–36}

The experimental study on PDAs reports the protonated states of the dendron moieties as a function of pH.11 Figure S1 shows the sequence of the PDA. The primary amines are located at the terminal ends of the branches. However, the tertiary amines are in the interior of the dendron branches. All branching points in the PAMAM dendron are tertiary amines. The primary (terminal groups) and tertiary amines (branching points) are connected with amide linkages. The pKa for primary and tertiary amines in PAMAM dendrons is \sim 9.2 and \sim 6.3, respectively. Hence, for acidic pH conditions (pH = 4), the experimental study on PDAs¹¹ reports that the primary and tertiary amines are protonated (unit positive charge). For basic pH conditions (pH = 10), none of the amines are protonated. The other groups on the branches (namely, the amide groups) are not protonated for any of the pH conditions. These protonation states are incorporated into the current study by changing the types of the MARTINI beads. These changes are guided by an earlier computational study on dendrimers.³⁶ The primary and tertiary amines are represented by the Q_d MARTINI beads when they are protonated. The primary amines are represented by the P₃ MARTINI bead when they are deprotonated. However, the tertiary amines are represented by the N₀ MARTINI bead when they are deprotonated. The amides are represented by the P3 MARTINI bead for all pH

The P₄ MARTINI beads are used to represent water molecules. 10% of the CG water beads are replaced with MARTINI antifreeze

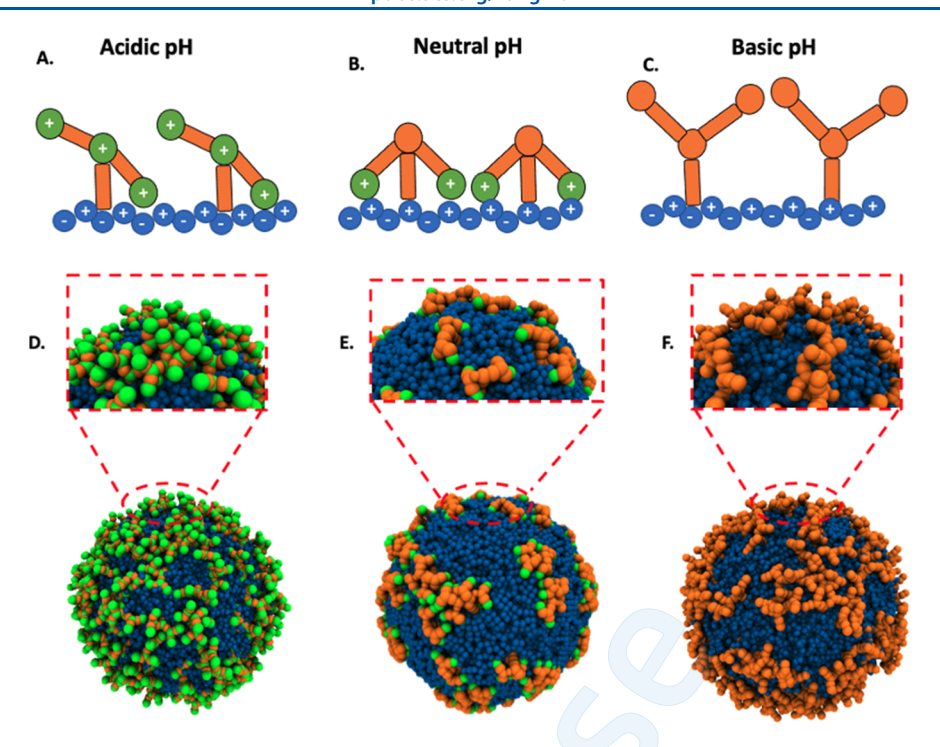


Figure 1. (A–C) Typical conformations adopted by dendron branches as a function of pH. Color scheme: green and orange beads represent charged and uncharged dendron groups, respectively. The lipid vesicle surface is represented by blue beads. The positively charged beads are choline groups, and the negatively charged beads are phosphate groups. (D–F) Zoomed-in views of a patch on the vesicle show the average dendron branch conformation.

beads to avoid freezing.³⁰ Chloride ions are inserted into the simulation box to maintain charge neutrality of the system. These ions are represented by the Q_a MARTINI bead.

A G5 dendrimer is used to validate the model with corresponding results from an earlier study.³⁶ The radius of gyration of a single G5 dendrimer for acidic, neutral, and basic conditions are measured. These measurements are in agreement with prior experimental⁴³ and computational³⁶ results (see Table S1).

A vesicle is created by starting with a flat lipid bilayer. A preassembled bilayer of dimensions $30 \times 30 \times 4$ nm³ is generated with a publicly available Python script.³³ The bilayer is placed in a three dimensional periodic simulation box of the same dimensions. The bilayer consists of 3040 DPPC lipids. The *z*-dimension of the simulation box is expanded from 4 to 10 nm. This is to accommodate water beads that will solvate the top and bottom surfaces of the bilayer. The sides of the bilayer interact with their own periodic image. This setup ensures that the bilayer is stable and flat. This initial configuration is energy minimized for 5000 steps using the steepest descent algorithm. The system is equilibrated in the NVT ensemble at a temperature of 323 K. Finally, a production run is performed in the NPT ensemble with semi-isotropic pressure coupling for 400 ns. Details of the thermostat and barostat are provided in an earlier study.²¹

A selected number of DPPC lipids in the bilayer are replaced by PDAs. This is carried out with the help of a grid that is overlaid on the bilayer that selects DPPC lipids on the upper and lower monolayer. The hydrophilic residues of these lipids are replaced with dendron moieties. This bilayer (encompassing PDAs and DPPC lipids) is equilibrated for another 400 ns using the NPT ensemble. The equilibrated bilayer is placed at the center of a large simulation box of dimensions $50 \times 50 \times 50 \text{ mm}^3$. The empty space in the box is filled with water beads. This setup exposes the hydrophobic alkyl chains along the edge of the bilayer to the hydrophilic solvent. The bilayer shields the hydrophobic groups from the hydrophilic solvent by reorganizing the amphiphiles at the edges. This results in the formation of a bicelle (Figure S2C). The bicelle further minimizes its interfacial energy by bending to fuse its edge and form a vesicle (Figure S2F). This system is simulated using the NPT ensemble

under isotropic pressure coupling for 4000 ns. Typically, the bilayer forms a vesicle within the first 1000 ns of the run. The final 100 ns of the simulation trajectory is used for analysis. A timestep of 20 femtoseconds is employed for all production runs. This process is also known as membrane fusion. To ensure reproducibility of the results, the simulations for each composition are repeated four times using randomly generated initial seeds. At higher dendron concentrations, the bicelle is unable to bend to form a stable vesicle (Figure S3). All simulation files are available in a public repository. 46

■ RESULTS AND DISCUSSION

The impact of key factors including interactions, excluded volume, concentration of PDAs, and the external environment on the self-organization of PDAs in a vesicle is investigated. The excluded volume of the PDAs is controlled via the dendron generation. The PAMAM dendron generation varied from 1 [generation 1 (G1)] through 5 (G5). To minimize the impact of the chemistry of the PDAs within the bilayer, the hydrophobic components of the PDAs and DPPC are identical. The external environment is varied via the pH. For this study, the pH values used are 4 and 10 for acidic and basic environments, respectively. For acidic pH conditions, the primary and tertiary amines of PAMAM are protonated (i.e., positively charged). For basic pH conditions, none of the amines are protonated. As a baseline, only the primary amines are protonated for neutral pH conditions.²¹ The polar head group in DPPC (namely, phosphocholine) remains zwitterionic under a wide range of pH values. 47,4

For acidic conditions, the positively charged primary and tertiary amine groups in neighboring PAMAM dendrons are expected to repel each other but have favorable electrostatic interactions with the negatively charged moieties on the phospholipid head group (Figure 1). This results in some of the dendrons pointing away from the surface, while other dendrons approach the surface. This configuration results in

lower numbers of interactions measured between the dendron branches (Figure 2). The effect of a higher concentration of

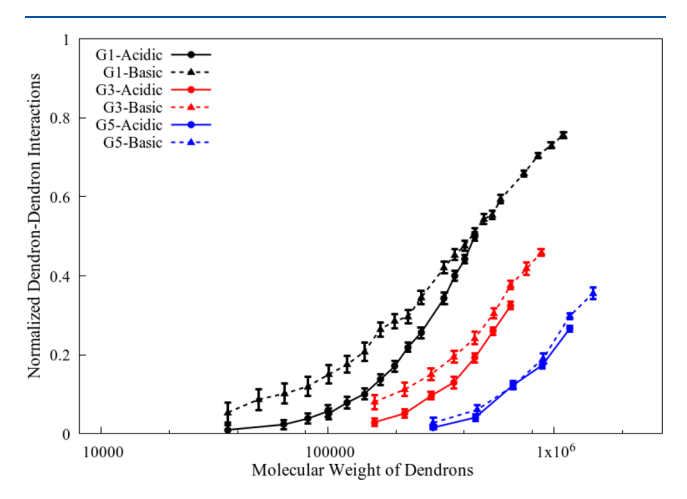


Figure 2. Interactions between the dendron branches for different generations, concentration of PDAs, and acidic and basic conditions. The number of interactions is normalized by the total number of possible dendron—dendron interactions. This measurement is performed for the dendrons on the outer surface of the vesicle. **Figure S6** shows the data for all generations (G1 through G5).

dendrons on this configuration will be discussed in a later section. In addition, the branches of neighboring dendrons have a lower degree of intermeshing (Figure S4A). The method of computing the degree of intermeshing between the dendron branches is explained in Figure S5. For basic pH conditions, the amines are unprotonated, resulting in the dendrons maximizing their conformational entropy by extending out into the aqueous medium away from the vesicle surface. Since there are no unfavorable interactions between the branches, higher concentrations of dendrons can be accommodated on the vesicle surface. As a consequence, the interactions between the dendron branches are always higher for basic conditions (Figure 2). Figure S4B shows that the branches of neighboring dendrons intermesh at high dendron concentrations for basic pH. Both of these observations suggest that dendrons favor interactions with neighboring dendrons and intermeshing of their branches when they are present at a higher concentration on the vesicle. For neutral pH, the positively charged terminal groups of the dendron branches interact with the negatively charged lipid head groups on the vesicle surface (i.e., the phosphate groups). These attractive electrostatic interactions induce the dendron branches to adopt conformations which allow the terminal groups to approach the vesicle surface (Figure 1).²¹

To better understand the degree of intermeshing of the branches, the conformation of the dendrons is investigated. For acidic conditions, the dendron branches have two responses to an increase in their relative concentration: (a) the branches extend away from the surface of the vesicle (see Figure S7) and (b) the branches slightly reduce their effective size (see Figure S8). These conformational changes minimize the intermeshing of the dendron branches (see Figure 3). At acidic pH, the intermeshing of dendron branches is unfavorable as it would result in electrostatic repulsions (primary and tertiary amines on the dendron branches are positively charged). Specifically, there are two types of unfavorable electrostatic interactions that arise under acidic

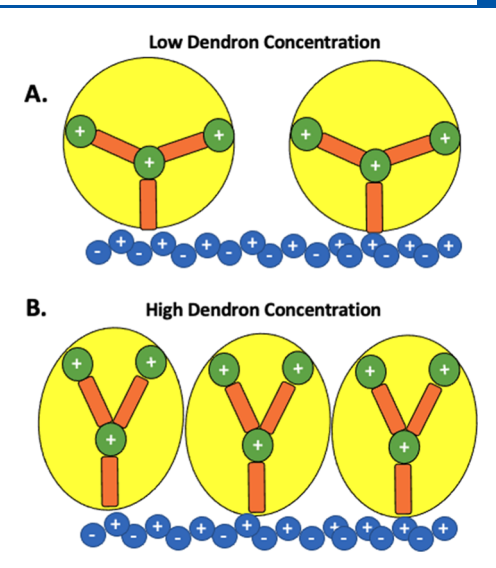


Figure 3. Change in the branch conformation as a function of dendron concentration. (A) Conformation of dendron branches at a low concentration. (B) Conformation of dendron branches at a high concentration. At higher concentrations, dendron branches increase their height and slightly reduce their effective size. These conformational changes minimize the intermeshing between neighboring dendron branches.

conditions. First, there are unfavorable electrostatic interactions between the neighboring dendrons (see Figure S9A). Second, there are unfavorable electrostatic interactions within the branches of individual dendrons (see Figure S9B). At higher concentrations, dendrons are positioned closer to each other. This will result in unfavorable interactions between the neighboring dendrons. Hence, it is surmised that the dendrons reduce their effective size. This change in conformation could reduce the lateral spacing between the dendrons, thereby minimizing the unfavorable interactions between the dendrons. However, if individual dendrons reduce their effective size, their own branches will be spatially close to each other. This could result in unfavorable interactions within the dendron. Hence, it is surmised that dendron branches increase their height. This change in conformation could increase the spacing between the charged groups in a dendron, thereby minimizing unfavorable interactions.

To characterize these conformational changes, the aspect ratio of the branches of individual dendrons (i.e., the ratio of the height to the radius of gyration of the dendron branches) is computed (see Figure S10). Table 1 shows the scaling exponent (α) for the aspect ratio as a function of the molecular weight of dendrons [i.e., aspect ratio \sim (molecular weight)]. The scaling exponent for G1 dendrons is slightly higher than all other dendron generations. This implies that

Table 1. Scaling Exponent (α) for the Following Relation: Aspect Ratio \sim (Molecular Weight)^a

generation	pН	scaling exponent (α)
1	acidic	0.29 ± 0.03
2	acidic	0.23 ± 0.02
3	acidic	0.24 ± 0.04
4	acidic	0.22 ± 0.05
5	acidic	0.24 ± 0.04

^aThese values are for all dendron generations at acidic pH.

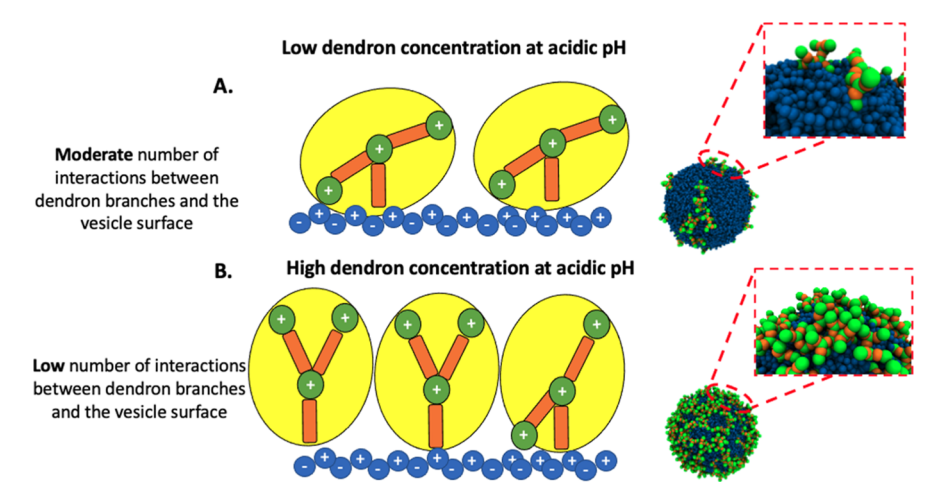


Figure 4. Dendron conformation as a function of the dendron concentration at acidic pH. At lower concentrations (A), there are a moderate number of interactions between the dendron branches and the surface of the vesicle. However, at higher concentrations (B), there are a lower number of interactions between the dendron branches and the surface of the vesicle. The dendron branches are flexible and hence change their conformation during the course of the MD simulation. Therefore, these schematics depict the average conformation adopted by the dendron branches.

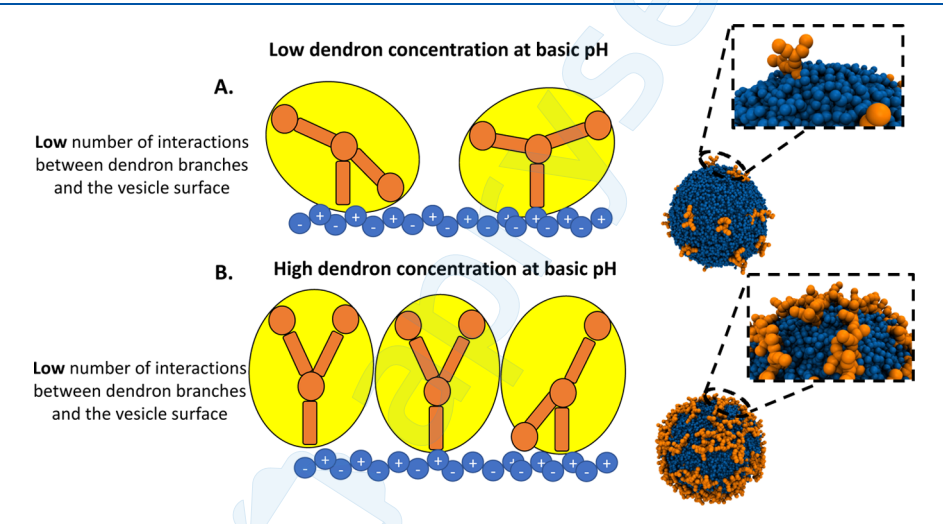


Figure 5. Conformation of dendrons as a function of their concentration at basic pH. For all concentrations (A,B), there are a low number of interactions between the dendron branches and the surface of the vesicle. The dendron branches are flexible and hence change their conformation during the course of the MD simulation. Therefore, these schematics depict the average conformation adopted by the dendron branches.

the change in the conformation of G1 dendrons is greater than the change in conformation of the higher generations. This result indicates that intermeshing of dendron branches is unfavorable for smaller generations (like G1) for acidic conditions. Figure S4A shows that G1 dendrons do not intermesh at higher dendron concentrations. However, higher generations intermesh their branches at higher concentrations. For basic pH conditions, the dendron branches do not show any systematic changes to an increase in their concentration (see Figure S10). However, the branches extend away from the surface of the vesicle at higher dendron concentrations. This change could be driven by excluded volume effects of the dendron branches, wherein individual dendron branches reorganize to occupy a volume that is not intruded upon by neighboring dendron branches.

For all dendron generations, the interactions between the dendron branches and the surface of the vesicle vary for acidic conditions (Figure S11). These interactions are observed to change with the concentration of the dendrons on the surface. These changes are driven by the need to minimize the

intermeshing of the dendron branches, thereby reducing the repulsive interactions between the branches. At lower dendron concentrations, the branches adopt conformations that increase their interactions with the surface of the vesicle (see Figure 4). It is surmised that these conformations increase the separation between the dendron branches, thereby reducing the repulsive interactions between them. However, at higher dendron concentrations, the interactions between the dendron branches and the surface of the vesicle are overwhelmed by the highly repulsive interactions between the closely spaced dendron branches (see Figure 4). The dendron branches move away from the surface of the vesicle, extending into the aqueous solution and thereby, increasing their height. As an aside, it is noted that all the dendron branches do not move away from the surface of the vesicle. A lower number of interactions between the dendron branches and the vesicle surface indicates that the branches move away from the surface of the vesicle. Figure S11 shows that the interactions between the dendron branches and the vesicle surface decrease for

higher dendron concentrations. However, the number of interactions does not become zero under any circumstances.

The dendron conformations adopted for basic pH are significantly different, as schematically represented in Figure 5. Interactions between the dendron branches and the surface of the vesicle are nearly constant as a function of the concentration (see Figure S11). A slight reduction in these interactions is observed at higher concentrations. These observations indicate that conformational changes are expected only at higher concentrations for basic pH, as confirmed in Figure S10. The conformational changes at higher concentrations are posited to occur due to excluded volume effects. Systems with G1 dendrons show exception to these trends, possibly on account of their low excluded volume.

Dendrons of larger generations have longer and more spread out branches which extend away from the surface of the vesicle for acidic pH, resulting in fewer interactions between the dendrons and the surface of the vesicle (Figure S11). The extended branches have the potential to result in intermeshing of neighboring branches in spite of the high number of like-charged moieties.

The number of dendrons on the outer monolayer of the vesicle is always higher than that on the inner monolayer (Figures S12 and S13). The distribution of dendrons across the two monolayers is measured by the asymmetric ratio, that is, the ratio of the number of dendrons on the outer monolayer to the number of dendrons on the inner monolayer (Figure S14). Larger dendron generations such as G5 are far more sensitive to changes in the asymmetric ratio as a function of the concentration. At higher concentrations, increasing number of dendrons prefer to be on the outer monolayer due to volumetric constraints of the vesicle cavity. The asymmetry in the number of dendrons across the two monolayers arises during the membrane fusion process when the dendrons spatially reorganize by diffusing and migrating from the inner to the outer monolayer. 21 Figure S14 shows the distribution of dendrons across the monolayers to be independent of the pH of the environment.

The total number of dendrons which can be accommodated on the surface of the vesicle, without destabilizing it, is constrained by the total area available on the outer surface of the vesicle. The maximum number of PDAs that can be accommodated in the vesicle bilayer while preserving its stability is termed as the threshold concentration, as shown in Figure 6. The projection of the dendron branches on the outer surface of the vesicle (namely, the projected surface area) at the threshold concentration is within the range of 90 and 100%

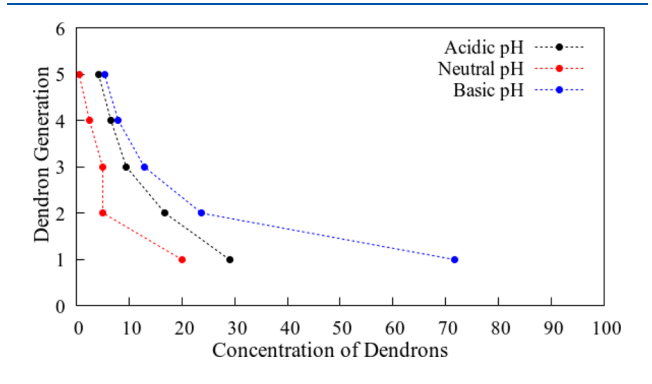


Figure 6. Threshold concentrations for all dendron generations as a function of pH.

(Figure 7). This means that the dendron branches occupy approximately 90–100% of the outer surface area of the

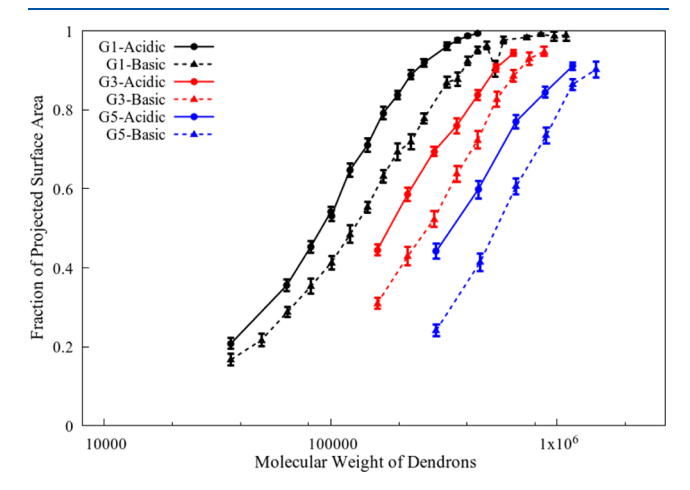


Figure 7. Fraction of projected surface area of dendron branches on the outer surface of the vesicle. The fraction of projected surface area is given by the ratio of the projected surface area to the total outer surface area of the vesicle. Figure S16 shows the data for all generations (G1 through G5).

vesicle. A higher number of PDAs with lower dendron generations (e.g., G1) fit within this range, thereby having higher threshold concentrations. However, PDAs with larger dendron generations (e.g., G5) have lower threshold concentrations.

The maximum projected surface area, or threshold area, of the dendrons on a stable vesicle is independent of generation and pH (Table 2), thereby demonstrating that the stability of the vesicle is dependent on the total projected area of dendrons.

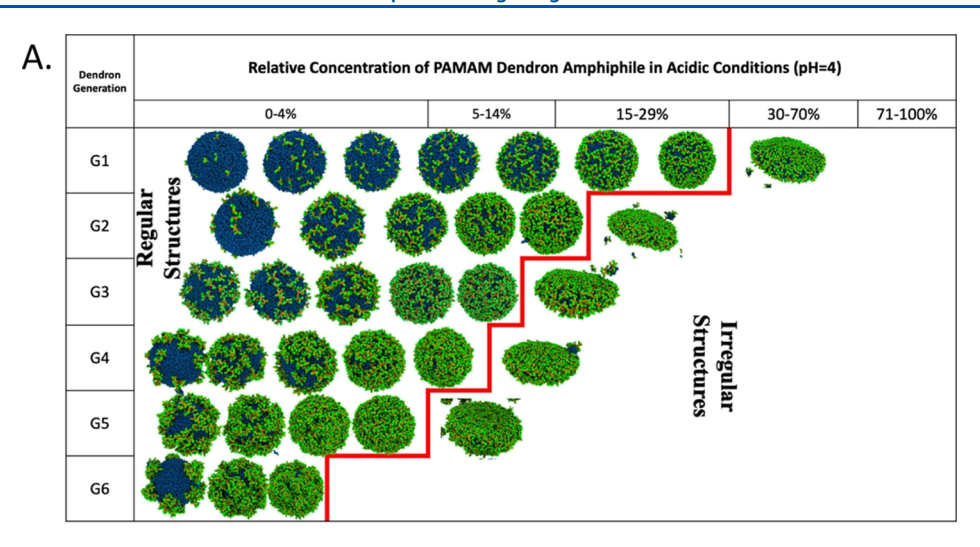
Table 2. Fraction of the Projected Surface Area of Dendron Branches at the Threshold Dendron Concentration^a

generation	acidic pH	basic pH
G1	0.993 ± 0.002	0.988 ± 0.014
G2	0.962 ± 0.022	0.974 ± 0.008
G3	0.943 ± 0.007	0.947 ± 0.011
G4	0.927 ± 0.009	0.939 ± 0.012
G5	0.911 ± 0.009	0.902 ± 0.019

^aA value of 1 means that the dendron branches occupy the entire outer surface of the vesicle.

For a given concentration of PDAs, the projected area of the dendron branches under acidic conditions is always greater than that corresponding to basic conditions (Figure 7) due to the electrostatic repulsions between the amine groups. A larger projected area would minimize the electrostatic repulsions. Since the maximum projected surface area is the same for both the pH conditions (Table 2), fewer number of dendrons are accommodated on the surface of the vesicle for the acidic condition. Hence, the threshold dendron concentrations for acidic conditions are consistently lower than those for basic conditions (Figure 6).

The difference between threshold concentrations for acidic and basic conditions reduces for larger generations (Figure 6). This observation can be explained by examining the degree of



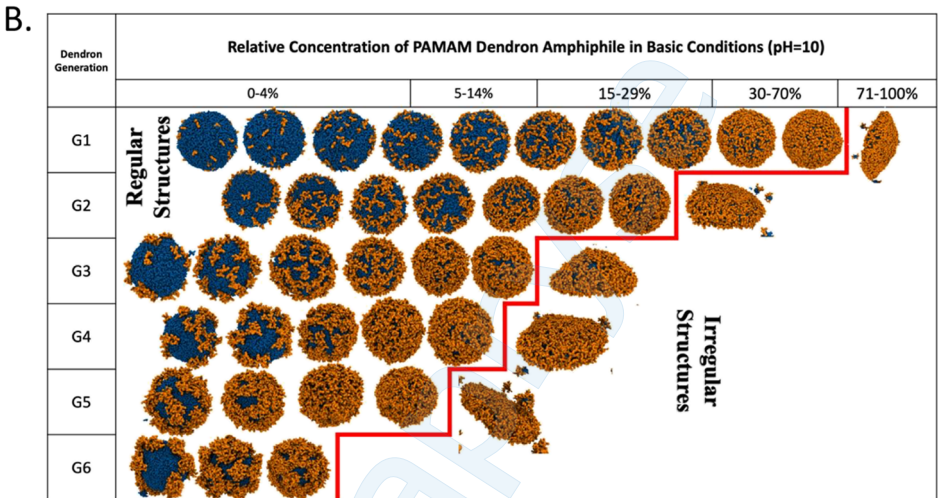


Figure 8. Phase diagram of the dendronized vesicles for acidic (A) and basic (B) pH conditions, as a function of the concentration of the PDAs and dendron generation. The regions, representative of the regular and irregular structures, are demarcated by the red line. Color scheme: blue—DPPC lipids, orange—uncharged dendron groups, and green—charged dendron groups.

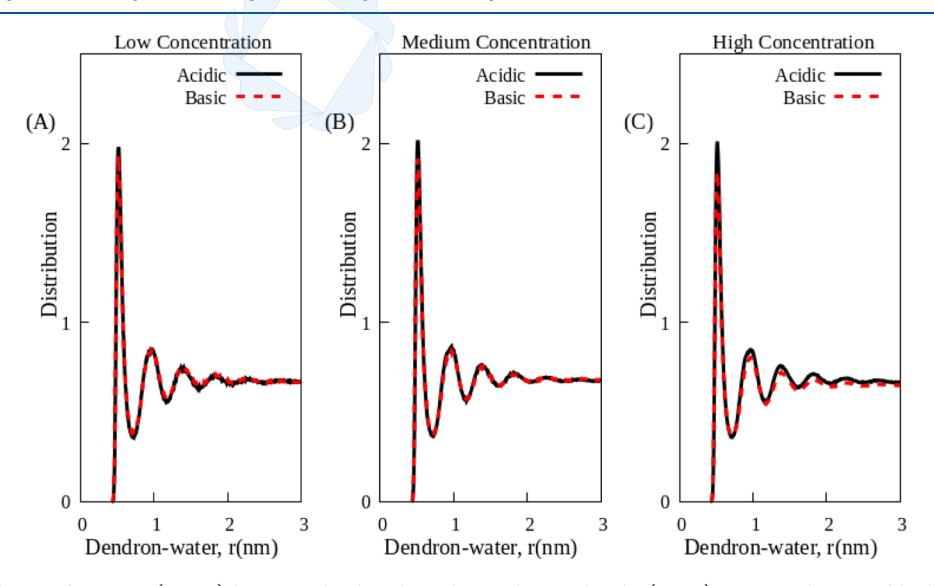


Figure 9. Radial distribution functions (RDFs) between dendron branches and water beads. (A–C) Low, medium, and high concentrations of G3 dendrons. The black and red curves correspond to acidic and basic pH conditions, respectively.

intermeshing between the dendron branches for the two pH conditions.

Since the total projected area that can be occupied by the dendron branches on the surface of the vesicle is fixed, a higher

degree of intermeshing between the branches will accommodate increasing concentrations of dendrons. For acidic conditions, the electrostatic repulsions limit the intermeshing of branches associated with dendrons of lower generations, thereby resulting in significantly smaller threshold concentrations (Figure S4A). However, for basic conditions, the lower generation dendron branches intermesh significantly at high concentrations (Figure S4B). For PDAs with larger dendron generations, the degree of intermeshing is nearly the same for the two pH conditions. For acidic conditions, there is significant intermeshing of the branches in spite of the higher number of positively charged moieties (Figure S15). It is surmised that this configuration is permitted as higher generation dendrons have fewer neighboring dendrons (Figure 2).

The formation of stable vesicles as a function of the generation and concentrations of PDAs under different external conditions is summarized in Figure 8. For both acidic and basic pH conditions, the threshold concentrations of PDAs are much higher than those for neutral pH.²¹ This result is attributed to the high number of interactions between the dendron branches and the surface of the vesicle at neutral pH (see Table S2). Favorable electrostatic interactions between the dendron branches and the surface of the vesicle give rise to the local intermonolayer asymmetric stresses, resulting in the rupture of the vesicle.^{21,35}

Figure 9 shows the coordination of solvent (water) with respect to the dendron branches. At basic pH, the water beads are slightly less coordinated with the dendron branches in comparison to that of acidic pH. This is mainly observed at a high dendron concentration. The radial distribution functions (RDFs) between the dendron branches and water beads are reported in Figure 9. This measurement is conducted for G3 dendrons at low (2.4%), medium (5.3%), and high (9.5%) relative concentrations. In the case of acidic pH, Figure 9 shows that the height of the first peak of the RDF (at ~0.5 nm) is constant for all concentrations. However, in the case of basic pH, the height of the first peak slightly reduces for higher concentrations. This means that under basic pH, any of the following scenarios could occur at higher dendron concentrations.

- a. The water beads are unable to penetrate the interior regions of the PAMAM dendrons.
- b. The dendron branches adopt conformations that minimize their interactions with water. For example, some branches could fold back into the interior region of the dendrons. This conformation has been observed in other all atom studies. 41,42 This phenomenon is referred to as back-folding.
- c. Both "a" and "b" could occur.

A more rigorous investigation is required to characterize the above three scenarios. However, this would require a model that better captures the interactions between water and dendron branches (such as hydrogen bonding). The current CG model cannot accurately study these interactions. In the future, a polarizable CG water model⁴⁹ could be employed to account for these interactions. It is noted that all atom studies of PAMAM dendrimers have investigated the impact of the solvent as a function of pH.^{41,42}

The findings of this study help in better understanding the characteristics of molecular assemblies such as pH-responsive liposomes. 1,11,50,51 For example, molecular assemblies that are

made up of PDAs are investigated in a previous experimental study. 11 Specifically, the study focused on assemblies consisting of G1 dendrons (these assemblies do not encompass DPPC lipids). At neutral and basic pH, stable vesicles are observed. These vesicles store drug molecules in their internal aqueous cavity. Upon delivery into the cytosol of the cell, the vesicles are destabilized, and the drug molecules are released. The destabilization of vesicles is attributed to the acidic conditions in the cytosol. Hence, the experimental study reports a drugdelivery strategy that is dependent on the pH-responsive behavior of vesicles. This study suggests that the pH-induced changes in the molecular shape of the PDA molecules could dictate the stability of the vesicles. Specifically, the study surmises that the size and extension (or height) of the dendron branches are larger at acidic pH. This could explain the destabilization of the vesicles at acidic pH. To better characterize the molecular details of dendrons that govern the stability of these systems, computational studies are required.

In the current computational study, dendronized vesicles encompassing a mixture of PDAs and DPPC lipids are reported. Although the components of the vesicles are different, the results for acidic and basic pH conditions can be compared to the findings of the previous experimental study. The current study demonstrates that dendronized vesicles are more stable under basic pH conditions. This is supported by the fact that the threshold concentration of dendrons that results in stable vesicles is always higher under basic conditions (see Figure 6). For example, in the case of G1 dendrons, the threshold concentration of dendrons is ~70% at basic conditions and ~30% at acidic conditions. Hence, these vesicles mimic the pH-responsive behavior of the vesicles reported by experiments. Furthermore, this study characterizes the size and height of the dendron branches as a function of pH. At any given relative concentration, the size and height of the dendron branches are larger at acidic pH. As suggested in the previous experimental study, 11 such changes in the molecular shape of the PDA molecules could be responsible for the destabilization of vesicles at acidic pH. Hence, these molecular insights could help in the design of pH-responsive assemblies with greater precision for drug-delivery applications.

CONCLUSIONS

Spherical surfaces decorated with mobile, solvophilic chains are found in nature in the form of cells bearing carbohydrate chains⁵² or encountered in biomedical sciences for drug delivery⁵³ and diagnostics.^{54,55} The physio-chemical properties of the chains determine their self-organization along with the functionality and stability of the spherical surfaces. For example, large and bulky solvophilic chains can stabilize spherical surfaces such as vesicles in aqueous solution.⁵ However, pH-responsive solvophilic chains can rupture vesicles under certain conditions. ^{11,21} In addition, the conformation of these chains can change significantly with concentrations, thereby impacting their organization and the stability of the spherical surfaces. This study elucidates the impact of four key factors (namely, the interactions, excluded volume, concentration of the chains, and the external environment) on the organization of these mobile, solvophilic chains on spherical surfaces, and its effect on the stability of the surfaces.

The study demonstrates that the self-organization of the dendrons on the surface of the vesicles differs for acidic and basic pH conditions. For acidic pH, neighboring dendron branches do not intermesh due to a high number of protonated dendron residues. To avoid intermeshing, the dendron branches undergo conformational changes that minimize interactions between the neighboring dendrons. These changes are not observed at basic pH due to the absence of protonated dendron groups. The differences in the results corresponding to acidic and basic pH conditions reduce for larger dendron generations. In spite of these differences, a significantly higher concentration of dendrons can be accommodated on the vesicles, without disrupting their stability, for both pH conditions. ²¹

The fundamental insights provided by this study can potentially advance diverse disciplines related to cell biology. S6-58 In addition, the vesicles examined in this study can be considered as model systems to predict the conformation of charged and uncharged biomolecules grafted to naturally occurring spherical assemblies such as exosomes. Furthermore, the results from this study can inform drug delivery strategies that depend upon external triggers such as pH for cargo release, such as cancer therapies and mRNA vaccine technologies.

ASSOCIATED CONTENT

Supporting Information

The Supporting Information is available free of charge at https://pubs.acs.org/doi/10.1021/acs.langmuir.2c03386.

Protonation states of a G1 PAMAM dendron-grafted amphiphile, validation of G5 dendrimer model, bilayer transitioning into a vesicle, bilayer failing to transition into a vesicle, intermeshing between neighboring dendron branches, interactions between the dendron branches for all generations, height of dendrons, effective size of dendrons, types of electrostatic repulsions, aspect ratio, interactions between dendron branches and the vesicle surface, distribution of dendrons in the vesicles, dendron generation plotted against molecular weight of dendrons, projected surface area data for all generations, and dendron—lipid interactions (PDF)

AUTHOR INFORMATION

Corresponding Author

Meenakshi Dutt — Chemical and Biochemical Engineering, Rutgers, The State University of New Jersey, Piscataway, New Jersey 08854, United States; orcid.org/0000-0001-5383-2992; Email: meenakshi.dutt@rutgers.edu

Author

Akash Banerjee — Chemical and Biochemical Engineering, Rutgers, The State University of New Jersey, Piscataway, New Jersey 08854, United States

Complete contact information is available at: https://pubs.acs.org/10.1021/acs.langmuir.2c03386

Notes

The authors declare no competing financial interest.

ACKNOWLEDGMENTS

The authors would like to acknowledge financial support from the NSF CAREER DMR-1654325 and OAC-1835449 awards. The authors would also like to acknowledge the use of computational resources supported by the NSF ACCESS (allocation DMR-140125) for portions of the research presented.

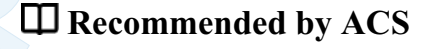
REFERENCES

- (1) Tenchov, R.; Bird, R.; Curtze, A. E.; Zhou, Q. Lipid Nanoparticles horizontal line From Liposomes to mRNA Vaccine Delivery, a Landscape of Research Diversity and Advancement. *ACS Nano* **2021**, *15*, 16982–17015.
- (2) Immordino, M. L.; Dosio, F.; Cattel, L. Stealth liposomes: review of the basic science, rationale, and clinical applications, existing and potential. *Int. J. Nanomed.* **2006**, *1*, 297–315.
- (3) Akbarzadeh, A.; Rezaei-Sadabady, R.; Davaran, S.; Joo, S. W.; Zarghami, N.; Hanifehpour, Y.; Samiei, M.; Kouhi, M.; Nejati-Koshki, K. Liposome: classification, preparation, and applications. *Nanoscale Res. Lett.* **2013**, *8*, 102.
- (4) Cheng, L.; Hill, A. F. Therapeutically harnessing extracellular vesicles. *Nat. Rev. Drug Discovery* **2022**, *21*, 379–399.
- (5) Mahendra, A.; James, H. P.; Jadhav, S. PEG-grafted phospholipids in vesicles: Effect of PEG chain length and concentration on mechanical properties. *Chem. Phys. Lipids* **2019**, 218. 47–56.
- (6) Ghosh, R.; Dey, J. pH-Responsive Vesicle Formation by PEGylated Cholesterol Derivatives: Physicochemical Characterization, Stability, Encapsulation, and Release Study. *Langmuir* **2020**, *36*, 5829–5838
- (7) Hashizaki, K.; Taguchi, H.; Itoh, C.; Sakai, H.; Abe, M.; Saito, Y.; Ogawa, N. Effects of poly(ethylene glycol) (PEG) chain length of PEG-lipid on the permeability of liposomal bilayer membranes. *Chem. Pharm. Bull.* **2003**, *51*, 815–820.
- (8) Moghimi, S. M. The effect of methoxy-PEG chain length and molecular architecture on lymph node targeting of immuno-PEG liposomes. *Biomaterials* **2006**, *27*, 136–144.
- (9) Yu, X.; Dutt, M. A multiscale approach to study molecular and interfacial characteristics of vesicles. *Mol. Syst. Des. Eng.* **2018**, *3*, 883–895
- (10) Yuba, E.; Nakajima, Y.; Tsukamoto, K.; Iwashita, S.; Kojima, C.; Harada, A.; Kono, K. Effect of unsaturated alkyl chains on transfection activity of poly(amidoamine) dendron-bearing lipids. *J. Controlled Release* **2012**, *160*, 552–560.
- (11) Doura, T.; Yamada, M.; Teranishi, R.; Yamamoto, Y.; Sugimoto, T.; Yuba, E.; Harada, A.; Kono, K. PAMAM Dendron Lipid Assemblies That Undergo Structural Transition in Response to Weakly Acidic pH and Their Cytoplasmic Delivery Capability. *Langmuir* **2015**, *31*, 5105–5114.
- (12) Aydin, F.; Uppaladadium, G.; Dutt, M. The design of shape-tunable hairy vesicles. *Colloids Surf.*, B **2015**, 128, 268–275.
- (13) Shinoda, W.; Discher, D. E.; Klein, M. L.; Loverde, S. M. Probing the structure of PEGylated-lipid assemblies by coarse-grained molecular dynamics. *Soft Matter* **2013**, *9*, 11549–11556.
- (14) Rud, O. V.; Polotsky, A. A.; Gillich, T.; Borisov, O. V.; Leermakers, F. A. M.; Textor, M.; Birshtein, T. M. Dendritic Spherical Polymer Brushes: Theory and Self-Consistent Field Modeling. *Macromolecules* **2013**, *46*, 4651–4662.
- (15) Lebedeva, I. O.; Zhulina, E. B.; Leermakers, F. A. M.; Borisov, O. V. Dendron and Hyperbranched Polymer Brushes in Good and Poor Solvents. *Langmuir* **2017**, *33*, 1315–1325.
- (16) Liu, P.; Chen, G.; Zhang, J. A Review of Liposomes as a Drug Delivery System: Current Status of Approved Products, Regulatory Environments, and Future Perspectives. *Molecules* **2022**, *27*, 1372.
- (17) Sercombe, L.; Veerati, T.; Moheimani, F.; Wu, S. Y.; Sood, A. K.; Hua, S. Advances and Challenges of Liposome Assisted Drug Delivery. *Front. Pharmacol.* **2015**, *6*, 286.
- (18) dos Santos Rodrigues, B.; Banerjee, A.; Kanekiyo, T.; Singh, J. Functionalized liposomal nanoparticles for efficient gene delivery system to neuronal cell transfection. *Int. J. Pharm.* **2019**, *566*, 717–730.
- (19) Han, X.; Zhang, H.; Butowska, K.; Swingle, K. L.; Alameh, M. G.; Weissman, D.; Mitchell, M. J. An ionizable lipid toolbox for RNA delivery. *Nat. Commun.* **2021**, *12*, 7233.

- (20) Fenton, O. S.; Kauffman, K. J.; McClellan, R. L.; Appel, E. A.; Dorkin, J. R.; Tibbitt, M. W.; Heartlein, M. W.; DeRosa, F.; Langer, R.; Anderson, D. G. Bioinspired Alkenyl Amino Alcohol Ionizable Lipid Materials for Highly Potent In Vivo mRNA Delivery. *Adv. Mater.* **2016**, 28, 2939–2943.
- (21) Banerjee, A.; Tam, A.; Dutt, M. Dendronized vesicles: formation, self-organization of dendron-grafted amphiphiles and stability. *Nanoscale Adv.* **2021**, *3*, 725–737.
- (22) Kneidl, B.; Peller, M.; Winter, G.; Lindner, L. H.; Hossann, M. Thermosensitive liposomal drug delivery systems: state of the art review. *Int. J. Nanomed.* **2014**, *9*, 4387–4398.
- (23) Ohtake, S.; Schebor, C.; de Pablo, J. J. Effects of trehalose on the phase behavior of DPPC-cholesterol unilamellar vesicles. *Biochim. Biophys. Acta, Biomembr.* **2006**, *1758*, 65–73.
- (24) Mohd, H. M. K.; Ahmad, A. F.; Radiman, S.; Mohamed, F.; Rosli, N. R. A. M.; Ayob, M. T. M.; Rahman, I. A. Interaction between silicon dioxide and dipalmitoylphosphatidylcholine (DPPC) vesicles. *AIP Conf. Proc.* **2014**, *1614*, 65–68.
- (25) Knecht, V.; Marrink, S.-J. Molecular Dynamics Simulations of Lipid Vesicle Fusion in Atomic Detail. *Biophys. J.* **2007**, *92*, 4254–4261.
- (26) Bennett, W. F. D.; Tieleman, D. P. Water Defect and Pore Formation in Atomistic and Coarse-Grained Lipid Membranes: Pushing the Limits of Coarse Graining. *J. Chem. Theory Comput.* **2011**, *7*, 2981–2988.
- (27) de Vries, A. H.; Mark, A. E.; Marrink, S. J. Molecular Dynamics Simulation of the Spontaneous Formation of a Small DPPC Vesicle in Water in Atomistic Detail. *J. Am. Chem. Soc.* **2004**, *126*, 4488–4489.
- (28) Nele, V.; Holme, M. N.; Kauscher, U.; Thomas, M. R.; Doutch, J. J.; Stevens, M. M. Effect of Formulation Method, Lipid Composition, and PEGylation on Vesicle Lamellarity: A Small-Angle Neutron Scattering Study. *Langmuir* **2019**, *35*, 6064–6074.
- (29) Park, Y.; Franses, E. I. Effect of a PEGylated Lipid on the Dispersion Stability and Dynamic Surface Tension of Aqueous DPPC and on the Interactions with Albumin. *Langmuir* **2010**, *26*, 6932–6942
- (30) Marrink, S. J.; Risselada, H. J.; Yefimov, S.; Tieleman, D. P.; de Vries, A. H. The MARTINI Force Field: Coarse Grained Model for Biomolecular Simulations. *J. Phys. Chem. B* **2007**, *111*, 7812–7824.
- (31) Darden, T.; York, D.; Pedersen, L. Particle mesh Ewald: An N-log(N) method for Ewald sums in large systems. *J. Chem. Phys.* **1993**, 98, 10089–10092.
- (32) Essmann, U.; Perera, L.; Berkowitz, M. L.; Darden, T.; Lee, H.; Pedersen, L. G. A smooth particle mesh Ewald method. *J. Chem. Phys.* **1995**, *103*, 8577–8593.
- (33) Wassenaar, T. A.; Ingólfsson, H. I.; Böckmann, R. A.; Tieleman, D. P.; Marrink, S. J. Computational Lipidomics with insane: A Versatile Tool for Generating Custom Membranes for Molecular Simulations. J. Chem. Theory Comput. 2015, 11, 2144–2155.
- (34) Lee, H.; Larson, R. G. Molecular Dynamics Simulations of PAMAM Dendrimer-Induced Pore Formation in DPPC Bilayers with a Coarse-Grained Model. *J. Phys. Chem. B* **2006**, *110*, 18204–18211.
- (35) Lee, H.; Larson, R. G. Lipid bilayer curvature and pore formation induced by charged linear polymers and dendrimers: the effect of molecular shape. *J. Phys. Chem. B* **2008**, *112*, 12279–12285.
- (36) Lee, H.; Larson, R. G. Effects of PEGylation on the Size and Internal Structure of Dendrimers: Self-Penetration of Long PEG Chains into the Dendrimer Core. *Macromolecules* **2011**, *44*, 2291–2298.
- (37) Cakara, D.; Kleimann, J.; Borkovec, M. Microscopic Protonation Equilibria of Poly(amidoamine) Dendrimers from Macroscopic Titrations. *Macromolecules* **2003**, *36*, 4201–4207.
- (38) Shao, N.; Su, Y.; Hu, J.; Zhang, J.; Zhang, H.; Cheng, Y. Comparison of generation 3 polyamidoamine dendrimer and generation 4 polypropylenimine dendrimer on drug loading, complex structure, release behavior, and cytotoxicity. *Int. J. Nanomed.* **2011**, *6*, 3361–3372.

- (39) Niu, Y.; Sun, L.; Crooks, R. M. Determination of the Intrinsic Proton Binding Constants for Poly(amidoamine) Dendrimers via Potentiometric pH Titration. *Macromolecules* **2003**, *36*, 5725–5731.
- (40) Pande, S.; Crooks, R. M. Analysis of Poly(amidoamine) Dendrimer Structure by UV–Vis Spectroscopy. *Langmuir* **2011**, 27, 9609–9613.
- (41) Maiti, P. K.; Goddard, W. A. Solvent Quality Changes the Structure of G8 PAMAM Dendrimer, a Disagreement with Some Experimental Interpretations. *J. Phys. Chem. B* **2006**, *110*, 25628–25632.
- (42) Maiti, P. K.; Çağın, T.; Lin, S.-T.; Goddard, W. A. Effect of Solvent and pH on the Structure of PAMAM Dendrimers. *Macromolecules* **2005**, *38*, 979–991.
- (43) Liu, Y.; Chen, C.-Y.; Chen, H.-L.; Hong, K.; Shew, C.-Y.; Li, X.; Liu, L.; Melnichenko, Y. B.; Smith, G. S.; Herwig, K. W.; et al. Electrostatic Swelling and Conformational Variation Observed in High-Generation Polyelectrolyte Dendrimers. *J. Phys. Chem. Lett.* **2010**, *1*, 2020–2024.
- (44) Bussi, G.; Donadio, D.; Parrinello, M. Canonical sampling through velocity rescaling. *J. Chem. Phys.* **2007**, *126*, 014101.
- (45) Parrinello, M.; Rahman, A. Polymorphic transitions in single crystals: A new molecular dynamics method. *J. Appl. Phys.* **1981**, *52*, 7182–7190.
- (46) Banerjee, A.; Dutt, M. Toolkit for automated construction and analysis of dendronized vesicles, 2022. https://github.com/duttm/Toolkit-for-automated-construction-and-analysis-of-dendronized-vesicles (accessed Feb 02 2023).
- (47) Marsh, D., Handbook of Lipid Bilayers. 2nd ed.; CRC Press, 2013. DOI:10.1201/b11712.
- (48) Wang, D. Y.; Yang, G.; Mei, H. C.; Ren, Y.; Busscher, H. J.; Shi, L. Liposomes with Water as a pH-Responsive Functionality for Targeting of Acidic Tumor and Infection Sites. *Angew. Chem., Int. Ed.* **2021**, *60*, 17714–17719.
- (49) Yesylevskyy, S. O.; Schäfer, L. V.; Sengupta, D.; Marrink, S. J. Polarizable water model for the coarse-grained MARTINI force field. *PLoS Comput. Biol.* **2010**, *6*, No. e1000810.
- (50) Karanth, H.; Murthy, R. S. R. pH-Sensitive liposomes-principle and application in cancer therapy. *J. Pharm. Pharmacol.* **2007**, *59*, 469–483
- (51) Zhao, Y.; Ren, W.; Zhong, T.; Zhang, S.; Huang, D.; Guo, Y.; Yao, X.; Wang, C.; Zhang, W.-Q.; Zhang, X.; et al. Tumor-specific pH-responsive peptide-modified pH-sensitive liposomes containing doxorubicin for enhancing glioma targeting and anti-tumor activity. *J. Controlled Release* **2016**, 222, 56–66.
- (52) Williams, C.; Royo, F.; Aizpurua-Olaizola, O.; Pazos, R.; Boons, G. J.; Reichardt, N. C.; Falcon-Perez, J. M. Glycosylation of extracellular vesicles: current knowledge, tools and clinical perspectives. *J. Extracell. Vesicles* **2018**, *7*, 1442985.
- (53) Guimarães, D.; Cavaco-Paulo, A.; Nogueira, E. Design of liposomes as drug delivery system for therapeutic applications. *Int. J. Pharm.* **2021**, *601*, 120571.
- (54) Tzror-Azankot, C.; Betzer, O.; Sadan, T.; Motiei, M.; Rahimipour, S.; Atkins, A.; Popovtzer, A.; Popovtzer, R. Glucose-Functionalized Liposomes for Reducing False Positives in Cancer Diagnosis. *ACS Nano* **2021**, *15*, 1301–1309.
- (55) Öztürk Öncel, M. Ö.; Garipcan, B.; Inci, F. Biomedical Applications: Liposomes and Supported Lipid Bilayers for Diagnostics, Theranostics, Imaging, Vaccine Formulation, and Tissue Engineering. In *Biomimetic Lipid Membranes: Fundamentals, Applications, and Commercialization*; Kök, F. N., Arslan Yildiz, A., Inci, F., Eds.; Springer International Publishing: Cham, 2019, pp 193–212.10.1007/978-3-030-11596-8 8.
- (56) Hamada, T.; Yoshikawa, K. Cell-Sized Liposomes and Droplets: Real-World Modeling of Living Cells. *Materials* **2012**, *5*, 2292–2305.
- (57) Fenz, S. F.; Sengupta, K. Giant vesicles as cell models. *Integr. Biol.* **2012**, *4*, 982–995.
- (58) Rampioni, G.; D'Angelo, F.; Leoni, L.; Stano, P. Gene-Expressing Liposomes as Synthetic Cells for Molecular Communication Studies. *Front. Bioeng. Biotechnol.* **2019**, *7*, 1.

- (59) Tenchov, R.; Sasso, J. M.; Wang, X.; Liaw, W.-S.; Chen, C.-A.; Zhou, Q. A. Exosomes—Nature's Lipid Nanoparticles, a Rising Star in Drug Delivery and Diagnostics. *ACS Nano* **2022**, *16*, 17802—17846.
- (60) Olusanya, T. O. B.; Haj Ahmad, R. R.; Ibegbu, D. M.; Smith, J. R.; Elkordy, A. A. Liposomal Drug Delivery Systems and Anticancer Drugs. *Molecules* **2018**, 23, 907.
- (61) Hou, X.; Zaks, T.; Langer, R.; Dong, Y. Lipid nanoparticles for mRNA delivery. *Nat. Rev. Mater.* 2021, 6, 1078–1094.



Role of Lipid Packing Defects in Determining Membrane Interactions of Antimicrobial Polymers

Samapan Sikdar, Satyavani Vemparala, et al.

MARCH 15, 2023 LANGMUIR

READ 🗹

Molecular Simulations on the Coalescence of Water-in-Oil Emulsion Droplets with Non-ionic Surfactant and Model Asphaltene

Xiaoyu Sun, Tian Tang, et al.

FEBRUARY 03, 2023

LANGMUIR

READ 🗹

Tween-80 on Water/Oil Interface: Structure and Interfacial Tension by Molecular Dynamics Simulations

Arthur Mussi Luz, Frederico Wanderley Tavares, et al.

FEBRUARY 24, 2023

LANGMUIR

READ 🗹

Study on the Bouncing Behaviors of a Non-Newtonian Fluid Droplet Impacting on a Hydrophobic Surface

Hailong Liu, Junfeng Wang, et al.

MARCH 10, 2023

LANGMUIR

READ 🗹

Get More Suggestions >